EGW 2014
3rd European Geothermal Workshop
Karlsruhe, 15-16 October 2014

Numerical Modeling of Borehole Heat Exchangers (BHEs) and its interactions with the surrounding soil

Haibing Shao[1,2], Sophie Schelenz[1,6], Norman Kist[3,1], Byoung Ohan Shim[4,1],
Anke Boockmeyer[6], and Olaf Kolditz[1,5]

[1]Helmholtz Centre for Environmental Research - UFZ, Leipzig, Germany
[2]Freiberg University of Mining and Technology, Freiberg, Germany
[3]Leipzig University of Applied Sciences - HTWK, Leipzig, Germany
[4]Korea Institute of Geoscience and Mineral Resources, Daejeon, South Korea
[5]Dresden University of Technology, Dresden, Germany
[6]Christian-Albrechts University, Kiel, Germany

Haibing.Shao@ufz.de

Keywords: Ground Source Heat Pump (GSHP); Shallow subsurface geothermal utilization; Borehole Heat Exchanger (BHE); OpenGeoSys

ABSTRACT

The utilization of Borehole Heat Exchanger (BHE) to transfer heat from the shallow subsurface has been a common practice for the Ground Source Heat Pump (GSHP) system. To represent realistic application scenarios for numerical simulations of such systems, saturated and unsaturated conditions as well as heterogeneous soil properties have to be considered. In this context, analytical solutions such as the Moving Finite Line Source (MFLS) model are not flexible enough to capture the full dynamics of the system. Furthermore, application examples with a high density of installed BHEs exist. There, temperature plumes produced by the individual BHEs may start to interact with each other and lead to lower thermal output.

To simulate this interaction, a dual continuum approach has been implemented into the open-source finite element simulator OpenGeoSys (OGS, www.opengeosys.org). The model is capable of simulating the temperature evolution both in and around the BHE, with the consideration of saturated and unsaturated groundwater flow processes in the surrounding soil. Instead of imposing Dirichlet or Neumann type of boundary conditions at the location of a BHE, the newly developed model allows the user to specify inflow refrigerant temperature and flow rate as the driving force of heat transport.

The extended OGS model was successfully verified by simulating an in-door thermal response test performed by Beier et al. (2011). The modeled BHE wall temperatures match perfectly with the measured values. The simulated outflow temperatures reproduce the same trend as monitored data, although with a small deviation (0.5°C). In the next step, the numerical model will be further applied in real geothermal sites including unsaturated soil layers and groundwater flow field.

1. INTRODUCTION

To describe the heat transport process in the surrounding soil of the Borehole Heat Exchanger (BHE), classical analytical solutions are available for saturated and homogeneous media. There are the infinite line source (ILS) model, the infinite cylindrical source (ICS) model, and the finite line source (FLS) model. Philippe et al. (2009) had a review on the validity ranges of these analytical models. When the groundwater flow has to be considered, then the Moving Finite Line Source (MFLS) model can also be adopted (Molina-Giraldo et al. 2011). These analytical solutions are then integrated together with numerical optimization algorithm, so that the best geometric arrangement and operation mode can be found for maximum energy extraction (Hecht-Mendez et al. 2013; Beck et al. 2013).

However, if the focus is on the short term temperature evolution in and around the BHE, then the numerical model must be adjusted to include the heat exchange between BHE and the surrounding soil (Kolditz et al. 2013). The conventional approach is to explicitly mesh the pipelines and grout zones in a BHE, then both the flow and heat transport process in the pipelines can be simulated (Focaccia 2013; Boockmeyer and Bauer 2014). This approach often requires refined mesh gird and small time step size, and leads to very long simulation time. The resolution of this issue was proposed by Al-Khoury et al. (2010), where a dual-continuum approach was adopted. The BHE, separated from the surrounding soil, was simulated as two different continuums and the heat flux between them is balanced through numerical iterations. This approach was recently adopted by Diersch et al. (2011a; 2011b), and implemented into the software FEFLOW (DHI-WASY 2010; Mielke et al. 2014). A study using FEFLOW shows that the analytical solution of Eskilson and Claesson (1988) cannot be used to simulate the temperature evolution in the staring period of BHE operation (less than 3.5 to 10 hours), when the thermal equilibrium has not been reached between the BHE and the surrounding soil.

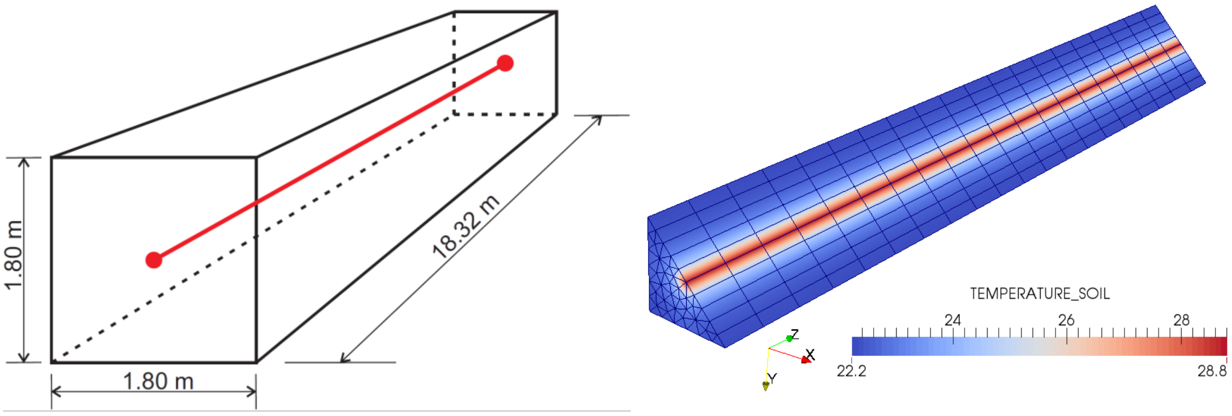

Figure 1: Geometry of the sandbox experiment (left) and simulated soil temperature distribution by OGS after 52 hours (right).

For the shallow geothermal systems, the challenge for the numerical model is to produce realistic prognosis of operational status of the entire ground source heat pump systems. This imposes two requirements on the model. 1) As the surrounding soil properties will have a great impact on the dynamics of heat transport, detailed information such as the groundwater table, groundwater flow direction and velocity, soil matrix porosity and conductivity must be obtained for the specific site and be integrated in the model. 2) The numerical model needs be further extended to include the BHE and the operation of heat pump systems behind as well. Then based on the required thermal load, prognosis can be made on meaningful operational parameters such as the coefficient of performance (COP) and electricity consumption. These parameters can be then optimized for specific site and leads to extensive investment and cost saving. In this work, we extend the feature of an existing open-source finite element simulator OGS (Kolditz et al. 2012) to simulate the interactions of BHEs and the surrounding soil, and verify the model against temperature measurements from an in-door thermal response test.

2. GOVERNING EQUATIONS

For the heat transport process in the soil, the development of soil temperature T_s is contributed by both the heat convection of the fluid *f* in the soil and the heat conduction through the soil matrix. Following Diersch (2014), let ρ^s, ρ^f, c^s, and c^f be the density and specific heat capacity of fluid *f* and soil *s*. If assuming the soil matrix is fully saturated with groundwater, the Darcy velocity can be described by the vector **q**, and the heat transport equation writes as

$$\frac{\partial}{\partial t}\left[\epsilon\rho^f c^f + (1-\epsilon)\rho^s c^s\right]T_s + \nabla\cdot\left(\rho^f c^f \mathbf{q} T_s\right) - \nabla\cdot\left(\Lambda^s \cdot \nabla T_s\right) = H_s, \tag{1}$$

with Λ^s the tensor of thermal hydrodynamic dispersion and H^s the source and sink terms for heat. When considering the heat exchange between the BHEs and the soil, the above governing equation is subject to a Cauchy-type of boundary condition:

$$q_{nT_s} = -(\Lambda^s \cdot \nabla T_s). \tag{2}$$

Inside the pipelines of a Borehole Heat Exchanger (BHE), depending whether it is the pipelines or the grout zones, the heat transport process is dominated by the convection of the refrigerant.

$$\rho^r c^r \frac{\partial T_k}{\partial t} + \rho^r c^r \mathbf{u}\cdot\nabla T_k - \nabla\cdot(\Lambda^r \cdot \nabla T_k) = H_k \quad \text{in } \Omega_k$$

with Cauchy type of BC: $-(\Lambda^r \cdot \nabla T_k)\cdot \mathrm{n} = q_{nT_k}$ on Γ_k, for $k = \mathrm{i1, o1(i2, o2)}$. (3)

Here Λ^r stands for the hydrodynamic thermal dispersion for the refrigerant, $\Lambda^r = (\lambda^r + \rho^r c^r \beta_L \,||\mathbf{u}||)\delta$. For the grout zones, the heat transport is mainly controlled by the heat dissipation.

$$\varepsilon^g \rho^g c^g \frac{\partial T_k}{\partial t} - \nabla\cdot(\varepsilon^g \lambda^g \cdot \nabla T_s) = H_k \quad \text{in } \Omega_k$$

with Cauchy type of BC: $-(\varepsilon^g \lambda^g \cdot \nabla T_k)\cdot \mathrm{n} = q_{nT_k}$ on Γ_k, for $k = \mathrm{g1, (g2, (g3, g4))}$ (4)

3. NUMERICAL SOLUTION AND IMPLEMENTATION

In order to simulate the heat transfer between BHEs and the surrounding soil, the governing equations for the pipeline and grout zones must be assemble into a global matrix system together with the linearized heat transport equation of the soil. When the equation (1) is combined with the matrix form of equation (3) and (4), the global matrix system writes as

$$\begin{pmatrix} P^s & 0 \\ 0 & P^\pi \end{pmatrix}\cdot\begin{pmatrix} \dot{T}^s \\ \dot{T}^\pi \end{pmatrix} + \begin{pmatrix} L^s - R^\pi & R^{s\pi} \\ R^{\pi s} & T^\pi \end{pmatrix}\cdot\begin{pmatrix} T^s \\ T^\pi \end{pmatrix} = \begin{pmatrix} W^s \\ W^\pi \end{pmatrix} \tag{5}$$

When Euler time discretization is applied on the above equation, the fully linearized global matrix system looks like

$$\begin{pmatrix} A^s & R^{s\pi} \\ R^{\pi s} & A^\pi \end{pmatrix}\cdot\begin{pmatrix} T^s \\ T^\pi \end{pmatrix}_{n+1} = \begin{pmatrix} B^s \\ B^\pi \end{pmatrix}_{n+1,n} \tag{6}$$

where *n* and *n+1* represents the previous and current time step. If a corrector recurrence scheme is applied, then the left-hand-side matrix and right-hand-side vectors write as

$$
\begin{aligned}
\boldsymbol{A}^{s} &= \frac{1}{\Delta t_n}\boldsymbol{P}^{s} + \theta(\boldsymbol{L}^{s} - \boldsymbol{R}^{\pi})\\
\boldsymbol{B}^{s} &= \left(\frac{1}{\Delta t_n}\boldsymbol{P}^{s} - (1-\theta)(\boldsymbol{L}^{s} - \boldsymbol{R}^{\pi})\right)\cdot T_n^{s} + W_{n+1}^{s}\theta + W_n^{s}(1-\theta)\\
\boldsymbol{A}^{\pi} &= \frac{1}{\Delta t_n}\boldsymbol{P}^{\pi} + \theta\boldsymbol{L}^{\pi}\\
\boldsymbol{B}^{\pi} &= \left(\frac{1}{\Delta t_n}\boldsymbol{P}^{\pi} - (1-\theta)(\boldsymbol{L}^{\pi})\right)\cdot T_n^{\pi} + W_{n+1}^{s}\theta + W_n^{s}(1-\theta) \qquad (7)
\end{aligned}
$$

where $\boldsymbol{P}$ and $\boldsymbol{L}$ stand for the assembled mass and Laplace matrices. After the $\boldsymbol{A}$ matrices and $\boldsymbol{B}$ vectors have been assembled, the OGS software employs a linear solver to calculate the temperature values $\boldsymbol{T}^{n+1}$ for the new time step, based on the previous time step value $\boldsymbol{T}^{n}$. Notice that, the heat exchange coefficients $\boldsymbol{R}^{\pi s}$ and $\boldsymbol{R}^{s\pi}$ will be multiplied with the temperature values, and producing the heat exchange flux between the soil and the BHE continuum, which is linearly dependent on the temperature difference. When a new set of temperature values are produced, the heat flux changes respectively. Therefore, a Picard iteration scheme has been employed in the OGS code, to solve for converged temperature values.

4. BENCHMARK RESULTS

For the FEFLOW software, the model was verified in two separate parts. For the BHE part, the results were compared against the Eskilson and Claesson (1988) analytical solution, assuming a fixed soil temperature. For the soil part, a fixed heat extraction rate was imposed on the BHE, and line source model was adopted for the verification. Such assumptions are not realistic in the field, because after the BHE runs for a while, the soil temperature surrounding it is going to be elevated, this will reversely influence how much heat will be extracted by the BHE. Recently, Beier et al. (2011) presented an in-door experiment, where the temperature evolution of both refrigerant and soil temperatures were monitored over a period of 52 hours with a one minute interval. Here in this work, we adopt the same experimental configuration and constructed our numerical model according to it.

As illustrated in Figure 1 (left), a 1.80×1.80×18.32 m sand box was constructed for the experiment. A single U-tube BHE was buried in the center of it. The initial temperature of the surrounding sand was measured at 22°C. A heater was installed in the loop of the refrigerant, so that a constant power of 1042 W was applied to the circulating fluid. As a result, the measured inflow temperature rose continuously over time (see the curve of black symbols in Figure 2, right). In our numerical model, we take the measured inflow temperature as boundary condition, and applied a constant refrigerant flow rate of 0.197 l/s. For parameters such as pipe radius, pipe distance, grout and pipe wall thermal conductivities, we adopted exactly the same values as in Beier et al. (2011). For the soil thermal conductivity, the independent probe measurement value of 2.82 W/(m K) was applied. The 3D simulation domain was spatially discretized into 20 line elements for the BHE and 2560 prisms for the soil. A fixed time step size of 21.6 seconds was applied for the simulation from 0 to 52 hours.

In the experiment, as the heater elevated the inflow temperature continuously, the outflow temperature rose accordingly. Figure 2 (left) compares the simulated temperature values against the measurements. In general, the trend of temperature evolution is successfully reproduced. A closer look at the profile from 10 to 52 hours shows a deviation of about 0.5°C in the outflow temperature. This can be caused by the approach regarding how the thermal resistance of grout zone is calculated in the numerical model. On the soil part, Figure 1 (right) demonstrates the simulated soil temperature distribution after 52 hours. At locations close to the center of the sand box, where the BHE is located, the soil temperature was elevated up to about 29°C. In Figure 3, the average soil temperature on the BHE wall is compared against the measured values, where a perfect match has been achieved. The BHEs are represented in the numerical model as line elements. This means they do not have an explicit cross section area. This can be the reason why the mean soil temperature produced by the model deviates away from the measurement at locations 24 cm away from the BHE wall (Figure 3, right).

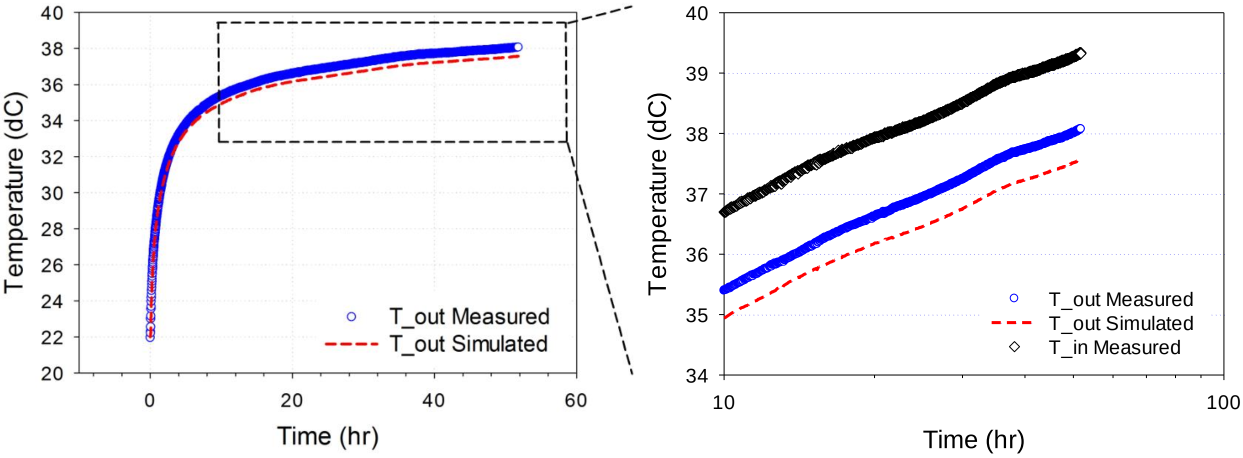

Figure 2: The simulated outflow temperature in comparison to the measured values. The left figure shows the entire profile from 0 to 51 hours, and the right figure focuses on the period after 10 hours, when the difference between inflow and outflow temperatures stabilizes.

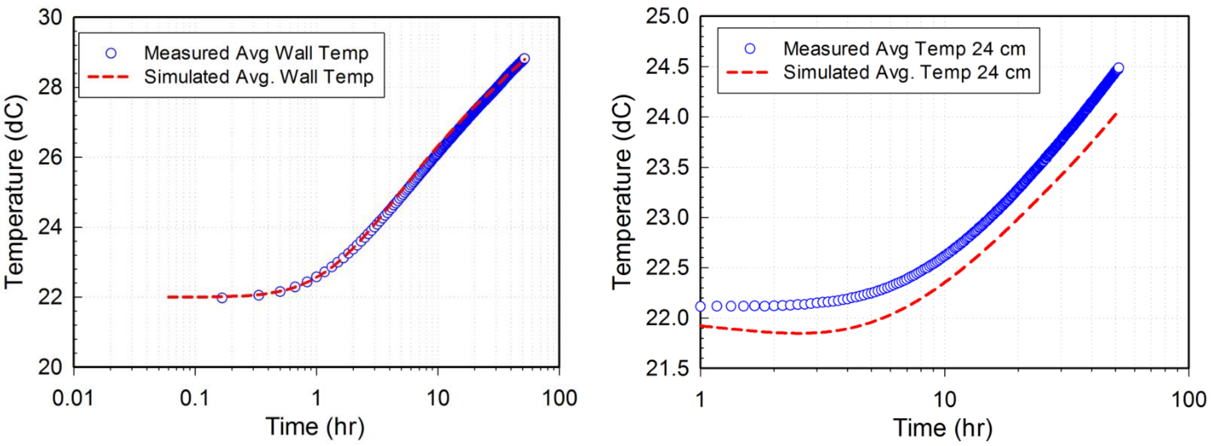

Figure 3: Comparison of measured and simulated soil temperature evolution at the borehole wall (left) and at 24 cm distance away from the BHE (right). The soil temperatures remain unaltered at 22 °C before 0.1 hours at the borehole wall (left) and 1 hour (right) at 24 cm distance.

5. CONCLUSIONS AND OUTLOOK

In this work, the numerical simulator OGS has been extended to simulate the thermal interaction between the borehole heat exchanger (BHE) and the surrounding soil. The extended feature has been successfully verified by simulating an in-door thermal response test by Beier et al. (2011). The code is capable of reproducing the same temperature evolution curve both for the circulating refrigerant and for the surrounding soil, despite of small deviations. The numerical code will be further applied to real geothermal sites, where unsaturated soil layers with groundwater flow processes are going to be considered.

REFERENCES

Al-Khoury R., Kölbel T., Schramedei R. (2010) Efficient numerical modeling of borehole heat exchangers, *Computers & Geosciences*, **36**(10): 1301-1315, DOI: 10.1016/j.cageo.2009.12.010.

Beck M., Bayer P., de Paly M., Hecht-Méndez J., Zell A. (2013) Geometric arrangement and operation mode adjustment in low-enthalpy geothermal borehole fields for heating, *Energy* **49**: 434-443, DOI: 10.1016/j.energy.2012.10.060.

Beier R. A., Smith M.D., Spitler J.D. (2011) Reference data sets for vertical borehole ground heat exchanger models and thermal response test analysis, *Geothermics* 40(1): 79-85, DOI: 10.1016/j.geothermics.2010.12.007.

Boockmeyer, A., Bauer, S. (2014). High-temperature heat storage in geological media: high-resolution simulation of near-borehole processes. *Géotechnique Letters* 4: 151–156. doi:10.1680/geolett.13.00060.

DHI-WASY (2010) FEFLOW finite element subsurface flow and transport simulation system-User's manual/reference manual/white papers. Recent release 6.0. DHI-WASY GmbH, Berlin. http://www.feflow.info

Diersch H.-J.G., Bauer D., Heidemann W., Rühaak W., Schätzl P. (2011a) Finite element modeling of borehole heat exchanger systems: Part 1. Fundamentals, *Computers & Geosciences* **37**(8): 1122-1135, DOI: 10.1016/j.cageo.2010.08.003.

Diersch H.-J.G., Bauer D., Heidemann W., Rühaak W., Schätzl P. (2011b) Finite element modeling of borehole heat exchanger systems: Part 2. Numerical simulation, *Computers & Geosciences* **37**(8): 1136-1147, DOI: 10.1016/j.cageo.2010.08.002.

Diersch H.-J.G. (2014) FEFLOW, Finite Element Modeling of Flow, Mass and Heat Transport in Porous and Fractured Media. Springer Heidelberg. DOI: 10.1007/978-3-642-38739-5.

Eskilson P., Claesson J. (1988) Simulation model for thermally interacting heat extraction boreholes. *Numerical Heat Transfer* **13**: 149-165.

Focaccia S. (2013) Thermal response test numerical modeling using a dynamic simulator. *Geothermal Energy* 1(3), DOI:10.1186/2195-9706-1-3.

Mielke P., Bauer D., Sebastian H., Annette G., Ingo S. (2014) Thermal effect of a borehole thermal energy store on the subsurface. Geothermal Energy 2(1), DOI: 10.1186/s40517-014-0005-1.

Hecht-Méndez J., de Paly M., Beck M., Bayer P. (2012) Optimization of energy extraction for vertical closed-loop geothermal systems considering groundwater flow, Energy Conversion and Management 66: 1-10, DOI: 10.1016/j.enconman.2012.09.019.

Kolditz O., Bauer S., Bilke L., Böttcher N., Delfs J.O., Fischer T., Görke U.J., Kalbacher T., Kosakowski G., McDermott C.I., Park C.H., Radu F., Rink K., Shao H., Shao HB., Sun F., Sun Y.Y., Singh A.K., Taron J., Walther M., Wang W., Watanabe N., Wu N., Xie M., Xu W., Zehner B. (2012): OpenGeoSys: an open-source initiative for numerical simulation of thermo-hydro-mechanical/chemical (THM/C) processes in porous media, *Environ. Earth Sci.*, **67**(2): 589-599, DOI: 10.1007/s12665-012-1546-x.

Kolditz O., Jakobs L. A., Huenges E., Kohl T. (2013) Geothermal Energy: a glimpse at the state of the field and an introduction to the journal. *Geothermal Energy* 1(1), DOI:10.1186/2195-9706-1-1.

Molina-Giraldo N., Blum P., Zhu K., Bayer P., Fang Z. (2011) A moving finite line source model to simulate borehole heat exchangers with groundwater advection, *International Journal of Thermal Sciences* **50**(12): 2506-2513, DOI: 10.1016/j.ijthermalsci.2011.06.012.